Bioscientia Medicina: Journal of Biomedicine and Translational Research
https://bioscmed.com e-ISSN: 2598-0580 Vol. 10, No. 4 (2026)

ORIGINAL ARTICLE

Diagnostic Accuracy and Optimal CD4 Threshold for Detecting Cytomegalovirus Retinitis in Advanced HIV Disease: A Prospective Indonesian Study

Petty Purwanita[1], Ramzi Amin[1*], Fadillah Amrina[1], Nuzulul Aini[1]

[1]Department of Ophthalmology, Faculty of Medicine, Universitas Sriwijaya/Dr. Mohammad Hoesin Central General Hospital, Palembang, Indonesia

ARTICLE INFO

Article history
Received: March 2, 2026
Accepted: April 1, 2026
Published: April 29, 2026

Keywords:
Cytomegalovirus retinitis
CD4 lymphocyte count
HIV
Sensitivity and specificity
ROC curve

**Corresponding author:*
Ramzi Amin
ramziamin20@gmail.com
ORCID: 0000-0003-1339-7580

DOI:
https://doi.org/10.37275/bsm.v10i4.1663

ABSTRACT

Background: Cytomegalovirus retinitis (CMVR) is a leading preventable cause of AIDS-related blindness where systematic screening is absent, and World Health Organization guidance triggers ophthalmic assessment below a CD4 count of 50–100 cells/µL, a range not previously calibrated in an Indonesian population.

Objective: To determine the diagnostic accuracy of the CD4 count against adjudicated cytomegalovirus retinitis, and to derive an optimal CD4 threshold for triggering ophthalmic screening, in Indonesian adults with advanced HIV disease.

Methods: This prospective single-gate diagnostic accuracy study, reported to STARD 2015, enrolled 51 consecutive adults with HIV-1 infection and a CD4 count below 100 cells/µL at Dr. Mohammad Hoesin Central General Hospital, Palembang, from January 2024 to January 2025. The index test was the CD4 count by flow cytometry; the reference standard was masked adjudication by two retina specialists using dilated ophthalmoscopy, fundus photography and optical coherence tomography (Cohen's $\kappa = 0.91$). Because only aggregated summaries were released, estimands the data do not identify are reported as sharp bounds.

Results: CMVR was present in 17 of 51 participants (33.3%, 95% CI 22.0–47.0); the median CD4 count was 17.0 cells/µL (IQR 11.0–27.0) versus 48.0 (30.0–72.0). The area under the ROC curve was 0.863 (95% CI 0.741–0.985). At the Youden-derived threshold of 32.5 cells/µL apparent sensitivity was 88.2% (95% CI 65.7–96.7) and specificity 91.2% (77.0–97.0); after correction for in-sample threshold selection these became 80.5% and 93.8%, and across two admissible reconstructions sensitivity ranged from 76.5% to 88.2%. CD4 rose monotonically across fulminant, indolent and frosted-branch phenotypes (bounded Kruskal–Wallis $p = 0.001–0.013$).

Conclusion: A CD4 count of approximately 30–35 cells/µL, with an unconditional visual-symptom over-ride, prioritises dilated retinal examination within the World Health Organization stratum in Indonesian HIV services.

1. Introduction

Cytomegalovirus retinitis (CMVR) is the most frequent sight-threatening opportunistic ocular infection in people living with human immunodeficiency virus (HIV) and, where systematic screening is absent, a leading preventable cause of AIDS-related blindness. An estimated 39.9 million people were living with HIV worldwide in 2023, of whom some 6.7 million reside in Asia and the Pacific, a region in which late diagnosis and delayed initiation of antiretroviral therapy (ART) sustain a large reservoir of advanced HIV disease.[1] Nationally representative surveys confirm that this reservoir has not closed despite treatment scale-up, with advanced HIV disease persisting in a substantial share of people living with HIV.[2] In Indonesia the pattern is extreme: across 19 referral hospitals in the INA-PROACTIVE cohort, 2,790 of 3,201 adults (87.2%) presented late, and the proportion did not fall in any year between 2015 and 2019,[3] while HIV prevalence at first test reaches 23.2% in some key populations in Jakarta.[4] Retention in care across South-East Asia is 75.2% (95% CI 66.7–82.1), and patients with a CD4 count of 200 cells/µL or above are more than twice as likely to remain in care.[5]

The pathogenesis of CMVR follows from the loss of CD4-dependent immune surveillance. Latent cytomegalovirus persists in myeloid progenitors and circulating monocytes; as CD4 T-lymphocyte help for virus-specific CD8 cytotoxic responses is lost, lytic reactivation occurs and the virus reaches the retinal vascular endothelium haematogenously. The immunological gradient is measurable in the blood: cytomegalovirus viraemia at the start of therapy correlates with a low CD4 count and a high HIV RNA level, and persistent viraemia predicts AIDS, serious non-AIDS events or death with an adjusted hazard ratio of 2.58 (95% CI 1.68–3.98),[6] while among 1,003 hospitalised adults with a median CD4 count of 33 cells/μL the prevalence of cytomegalovirus DNAaemia reached 39.8% (95% CI 36.7–42.9).[7] Endothelial infection produces full-thickness retinal necrosis with a sharply demarcated advancing border, occlusive vasculitis and breakdown of the blood–retinal barrier, and the formal classification criteria for CMVR, derived by machine learning on 803 cases of infectious posterior and panuveitis, achieve 93.3% accuracy (95% CI 88.2–96.3) on validation.[8] Three morphological phenotypes are recognised — a fulminant haemorrhagic variant, an indolent granular variant, and frosted branch angiitis, in which dense perivascular sheathing reflects a comparatively preserved immune response to viral antigen — and immune status is a determinant of phenotype and of the risk of retinal detachment.[9]

Current World Health Organization guidance recommends ophthalmic assessment, and consideration of pre-emptive anti-cytomegalovirus strategies, for patients with advanced HIV disease and a CD4 count below 50–100 cells/μL.[10] The threshold is pragmatic rather than empirically derived. Meta-analysis of 236 studies and 20,214 patients with AIDS-related CMVR found that 78% had a CD4 count below 50 cells/μL at diagnosis, that 44% had bilateral disease and that 29% were asymptomatic at presentation,[11] the last figure being the strongest single argument for screening rather than symptom-driven referral. Ocular involvement in HIV is common and CD4-dependent: 28.9% of 401 Ethiopian adults had ocular manifestations, with a CD4 count below 200 cells/μL carrying 4.76-fold increased odds,[12] posterior-segment lesions cluster at lower counts in Indian cohorts,[13] and retinal rather than anterior-segment involvement is the specifically CD4-dependent phenotype.[14] Reported CMVR frequency nevertheless varies enormously with the denominator used, from 1.7% among hospitalised Brazilian patients with a CD4 count of 100 cells/μL or below screened systematically,[15] through 7.7% among patients selected by cytomegalovirus viraemia,[16] to 8.5% of all people living with HIV at a Jakarta tertiary hospital, where one-year mortality after cytomegalovirus disease reached 27.2%.[17]

Diagnosis rests on masked ophthalmoscopic adjudication supported by fundus photography and optical coherence tomography, which resolves structural and microvascular damage extending beyond the visible lesion,[18] and by ultra-widefield imaging, which detects asymptomatic disease that systemic virology misses.[19] Alternative screening pathways are advancing quickly: teleretinal screening achieves a pooled sensitivity of 87.11% (95% CI 50.35–100) and specificity of 97.73% (95% CI 89.88–100),[20] machine-learning analysis of single-field photographs reaches 88.2% sensitivity for sight-threatening zone 1 disease,[21] and a deep-learning system applied to ultra-widefield images attains an area under the curve of 0.945 (95% CI 0.929–0.962).[22] Each of these, however, requires a camera, a trained operator and a reading pathway. Laboratory surrogates fare less well: plasma cytomegalovirus viral load agreed with the ophthalmic diagnosis in only 75% of cases in one series, with four retinitis cases having undetectable viraemia,[23] and intraocular polymerase chain reaction, although accurate at 82% sensitivity and 91% specificity, requires a paracentesis.[24]

Dr. Mohammad Hoesin Central General Hospital is the principal tertiary referral hospital for South Sumatra, serving a catchment of approximately 8.6 million people, and is the teaching hospital of the Faculty of Medicine, Universitas Sriwijaya. Its co-located HIV and ophthalmology services, with on-site flow cytometry and optical coherence tomography, make it one of the few Indonesian centres where a prospective diagnostic accuracy study of CMVR can be conducted with a complete and consistently applied reference standard. The practical question facing the service is not whether the CD4 count is associated with CMVR, which is not in doubt, but where within the already high-risk stratum below 100 cells/μL finite retina-specialist capacity should be concentrated. Point-of-care CD4 testing is scalable in comparable settings,[25] although its specificity in routine Indonesian and Ethiopian use is only 32.7% (95% CI 27.9–37.8), which constrains how such a rule could be deployed outside laboratories with flow cytometry.[26]

No prospective study from Indonesia has reported the diagnostic accuracy of the CD4 count for CMVR using receiver operating characteristic methodology, and none from the region has quantified the relationship between the CD4 count and CMVR morphological phenotype. This study was therefore designed with three specific aims: to estimate the prevalence of CMVR among consecutive patients with advanced HIV disease at a tertiary Indonesian centre; to determine the discriminative performance of the CD4 count and derive the threshold maximising the Youden index, comparing it formally with the World Health Organization threshold of 50 cells/μL; and to characterise the association between the CD4 count and CMVR morphological phenotype. Beyond these clinical aims, the analysis was designed to be explicit about what aggregate summary data can and cannot identify, so that every reported quantity is either exactly reproducible or accompanied by sharp bounds.

2. Methods

Study design and reporting

This was a prospective, single-gate diagnostic accuracy study conducted and reported in accordance with the Standards for Reporting of Diagnostic Accuracy Studies (STARD 2015) statement.[27] The design and its potential biases were additionally appraised against the four QUADAS-2 domains of patient selection, index test, reference standard, and flow and timing. The complete participant pathway, from screening through to the cross-classification of index test against reference standard, is set out in Figure 1. A single-gate design was chosen deliberately: participants were enrolled on a clinical indication, namely advanced HIV disease, rather than on their reference-standard result, so the resulting estimates apply to the population in which the rule would actually be deployed.

Setting

The study was conducted at the Department of Ophthalmology and the HIV service of Dr. Mohammad Hoesin Central General Hospital, Palembang, South Sumatra, Indonesia, a government tertiary referral hospital and the teaching hospital of the Faculty of Medicine, Universitas Sriwijaya, serving a regional population of approximately 8.6 million. The institution maintains an on-site clinical flow-cytometry laboratory and a medical retina service equipped for fundus photography and spectral-domain optical coherence tomography. Recruitment ran from January 2024 to January 2025 inclusive.

Participants and sampling

Consecutive adults attending the HIV or ophthalmology services were screened. Inclusion criteria were serologically confirmed HIV-1 infection, a CD4 lymphocyte count below 100 cells/μL, age 18 years or above, capacity to give written informed consent, and availability for a complete ophthalmic examination. Exclusion criteria, all applied before the index test was read, were treatment with ganciclovir, foscarnet or cidofovir within the preceding 12 months; previously documented immune-recovery uveitis attributable to CMVR; media opacity precluding an adequate view of the peripheral retina; and concurrent systemic cytomegalovirus disease requiring active treatment. The exclusions and the resulting analysed sample are shown in Figure 1. Consecutive sampling was used throughout the recruitment window to minimise selection bias; no participant approached declined, and no participant was lost between the index test and the reference standard, so the analysed sample equals the enrolled sample.

Sample size

The a priori calculation used the two-sample comparison-of-means formula for a case-control diagnostic design, $n_{case} = (Z_{1-\alpha/2} + Z_{1-\beta})^2 \times \sigma^2 \times (1 + 1/k) / \delta^2$, with $\alpha = 0.05$, $\beta = 0.10$, an assumed standard deviation σ of 5.15 cells/μL, a target difference δ of 4.0 cells/μL and a case-to-control ratio k of 1:2; the investigators recorded a requirement of 17 cases and 34 controls. We re-executed this calculation and note for transparency that the stated inputs in fact return 27 cases and 54 controls, the discrepancy arising because the assumed standard deviation is an order of magnitude smaller than the dispersion actually observed. We therefore treat the achieved sample as a fixed constraint and characterise the design by its realised precision: with 17 cases and 34 controls the half-width of the 95% Wilson interval for sensitivity is 15.5 percentage points and for specificity 10.0 percentage points, and the design retains 80% power to reject an area under the curve of 0.5 for any true area of 0.736 or greater.

Index test

The CD4 lymphocyte count was measured by flow cytometry (FACSCalibur, BD Biosciences, San Jose, CA, USA) on venous blood drawn within 48 hours of the ophthalmic examination and analysed in the institutional clinical laboratory under routine internal and external quality control. Results were reported as an absolute count in cells/μL. Laboratory staff were not informed of the ocular findings and the retina specialists performing the reference standard were not informed of the CD4 result, so masking was bidirectional. The candidate thresholds examined — 25, 30, 32.5, 35, 40 and 50 cells/μL — were specified before the accuracy analysis and span the World Health Organization decision range.

Reference standard

The reference standard was consensus adjudication of CMVR by two retina specialists with subspecialty experience in infectious uveitis, each masked to the CD4 result and to each other's assessment, applying the published classification criteria for cytomegalovirus retinitis.[8] Every participant underwent best-corrected visual acuity measurement on Snellen charts converted to the logarithm of the minimum angle of resolution (logMAR), slit-lamp biomicroscopy of the anterior segment with grading of cells and flare, indirect ophthalmoscopy through a dilated pupil using 78-dioptre and 90-dioptre non-contact lenses, colour fundus photography (TRC-50DX, Topcon, Tokyo, Japan) and spectral-domain optical coherence tomography (Triton Plus, Topcon). Pupillary dilatation used tropicamide 1% with phenylephrine 2.5%, and examination followed at least 20 minutes later. The full protocol is summarised in Figure 1.

CMVR was diagnosed when all of the following were present: granular or haemorrhagic retinal opacification in a perivascular distribution; a sharply demarcated border between involved and uninvolved retina; documented progression on serial examination at an interval of two to four weeks; and an absence of the dense, vision-obscuring vitritis that characterises acute retinal necrosis. Low-grade vitritis of 1+ or less is compatible with CMVR and was recorded in six participants, as reported in Table 1. Acute retinal necrosis, progressive outer retinal necrosis and other opportunistic retinopathies were excluded on the combined clinical, photographic and tomographic evidence, since optical coherence tomography resolves structural and microvascular damage that clinical inspection alone does not.[9,18] Agreement between the two adjudicators before consensus was excellent (Cohen's $\kappa = 0.91$, 95% CI 0.83–0.99), corresponding to at most approximately five of the 51 participants on whom the readers initially differed. Aqueous polymerase chain reaction, which has a sensitivity of 82% and a specificity of 91% for infectious uveitis, was not available and was not performed.[24]

Morphological phenotype was assigned by the same masked adjudication as fulminant (rapid centrifugal spread with confluent haemorrhage and dense opacification), indolent (slow centripetal progression with a granular leading edge and minimal haemorrhage) or frosted branch angiitis (dense perivascular arteriolar sheathing with comparatively limited necrosis), following the published classification and phenotype descriptions.[8,9] The Holland zone of involvement was recorded at examination but was not released in the aggregated dataset available for this analysis, so no zone-stratified result can be presented; this matters because zone 1 lesions predict worse visual acuity, more injections and more complications in randomised data.[28] Agreement was assessed formally for the diagnosis but not for the phenotype assignment, which is the more subjective judgement; any phenotype misclassification would attenuate rather than create the CD4 gradient reported below.

Data available for analysis and the recovery strategy

Analyses were performed on the aggregated cross-tabulations and group summary statistics generated by the study team; participant-level records were not released for secondary analysis under the institutional data-governance policy. Every categorical comparison reported in Table 1 is therefore exactly recoverable, because a count and a denominator determine a two-by-two table uniquely, whereas the CD4 count itself is available only as group quantiles and as the number of participants either side of each of six prespecified thresholds, that is, as an interval-censored variable. The reconstructed interval counts are displayed in Figure 2.

Three consequences follow and were handled explicitly. First, quantities that are functions of the two-by-two tables — sensitivity, specificity, predictive values, likelihood ratios, diagnostic odds ratios and net benefit — are point-identified and were computed exactly. Second, the area under the ROC curve is not point-identified by a single operating point; sharp lower and upper bounds were therefore derived by assigning the most and the least favourable possible ordering to every pair of participants lying on the same side of the cut-off, and were supplemented by a within-bin resampling estimate in which 20,000 replicate reconstructions were drawn uniformly within each observed CD4 interval. These are replicate reconstructions of the unobserved values, not bootstrap resamples of participants, and the resulting interval therefore excludes sampling variability; both are plotted in Figure 3. Third, quantities requiring the joint distribution of several covariates were not estimated at all; the refusals are listed in full in the Results.

Because a single-threshold rule is nested, the count of test positives can only increase as the threshold rises. The reported threshold series was therefore checked for monotonicity and, where it was violated, reconciled by isotonic regression using the pool-adjacent-violators algorithm, which returns the least-squares-closest monotone series and is the standard non-parametric remedy for an order-constrained estimate. Reported and reconciled series are shown side by side in Table 2.

Statistical analysis

Prevalence and all proportions are reported with 95% Wilson score intervals, which retain nominal coverage at small denominators and at proportions near the boundary; Clopper–Pearson intervals were computed in parallel and are reported where they differ by more than one percentage point. Between-group comparisons of categorical variables used Fisher's exact test, the exact conditional (Cornfield) odds ratio with its exact interval, the risk difference with its asymptotic interval, and Cramér's V with the Bergsma bias correction as the effect-size measure; because the two-by-two tables here are sparse, the conditional rather than the sample odds ratio is reported throughout. Nine baseline comparisons were made, so false-discovery-rate q values were computed by the Benjamini–Hochberg procedure and are reported beside every nominal p value in Table 1. Exact p values are given to three decimal places; values below 0.001 are reported as $p < 0.001$ because three-decimal reporting cannot represent them.

Discriminative performance was summarised by the area under the ROC curve, plotted in Figure 3, with the DeLong interval, which was verified against the Hanley–McNeil variance estimator for 17 cases and 34 controls. The optimal cut-off was that maximising the Youden index, J = sensitivity + specificity − 1. At the derived cut-off we report sensitivity, specificity, positive and negative predictive values, overall accuracy, positive and negative likelihood ratios with Katz logarithmic intervals, the diagnostic odds ratio, the F1 score and the Matthews correlation coefficient, all collected in Table 3.

Because the cut-off was chosen to maximise the Youden index in the same 51 observations in which it is evaluated, the apparent sensitivity, specificity and Youden index are upward-biased estimates of the performance the same rule would achieve in new data. An Efron–Gong optimism correction was therefore applied: within each of 200 reconstructed datasets, 100 bootstrap resamples were drawn, the threshold was re-derived in each resample and evaluated on the original reconstruction, and the mean difference was subtracted from the apparent value. Both apparent and optimism-corrected estimates appear in Table 3, and the apparent values are labelled as such throughout.

Coarse calibration is reported in Table 4 as the observed proportion with retinitis within each reconstructed CD4 interval, with Wilson intervals, because a clinician needs a risk gradient and not only a single cut-point. Predictive values were recomputed across a pre-test probability range of 5% to 40%, also in Table 4, to make their transportability explicit. An uncertainty budget at the foot of the same table reports separately the half-width attributable to sampling error, the spread attributable to the choice between two admissible reconstructions of the source data, and the optimism attributable to in-sample threshold selection; no formal combination of the three is claimed, and every interval estimate reported below is conditional on the adopted reconstruction.

Because a Youden-optimal cut-off implicitly weights a missed case and a false alarm equally, which is untenable when the missed condition is blinding and when randomised data show that lesion location at presentation determines visual outcome,[28] the expected-loss-minimising threshold was also computed as r × prevalence × (1 − sensitivity) + (1 − prevalence) × (1 − specificity) for relative costs r of a false negative to a false positive of 1, 3, 5, 10 and 20; the results are given in Table 5.

The joint distribution of the CD4 rule and visual-symptom status is not identified by the released summaries, so the accuracy of any logical combination of the two was bounded rather than estimated using the Fréchet–Hoeffding inequalities and is reported in Table 5.

Predictive values were recomputed across a pre-test probability range of 5% to 40% to make their transportability explicit and are plotted in Figure 4. Clinical usefulness was quantified by decision-curve analysis, in which net benefit = true positives/n − (false positives/n) × $p_t/(1 - p_t)$ across referral threshold probabilities p_t from 5% to 70%, with "examine all" and "examine none" as reference strategies. The derived threshold was compared with the World Health Organization threshold of 50 cells/µL by exact McNemar test on the raw integer counts; because the two rules are strictly nested, discordance is one-sided and fully determined by the difference in the number classified positive, so no assumption about pairing was required. The minimum attainable p value for the observed number of discordant pairs is reported alongside the p value itself.

Two quantitative bias analyses were prespecified. Because the reference standard was clinical rather than molecular, apparent accuracy was corrected for an imperfect reference standard under the assumption of conditional independence, solving the three-parameter system for true prevalence, true sensitivity and true specificity across a grid of assumed reference sensitivity from 0.85 to 1.00 and reference specificity from 0.95 to 1.00. Conditional independence is unlikely to hold exactly here: a participant with a very low CD4 count is more likely to have florid, unambiguous retinitis and therefore to be classified correctly by the reference standard, which is positive conditional dependence and biases the corrected sensitivity upward, so the corrected values should be read as optimistic. Because the study is observational, the minimum strength of unmeasured confounding capable of explaining away the diagnostic contrast was quantified by the E-value on the risk-ratio scale, using the rare-outcome approximation adjusted for the observed prevalence; it is reported in Table 5. A spectrum analysis re-weighted the reference-negative arm to simulate fuller representation of the 50–100 cells/µL stratum.

Association between the CD4 count and morphological phenotype was assessed by the Kruskal–Wallis test. Because only phenotype-specific medians and quartiles were available, the test statistic was not point-identified; it was bounded by exhaustive enumeration of all 585 rank allocations compatible with two stated constraints — that the four frosted-branch observations occupy the four highest ranks, which follows from the reported quartiles under the weighted-average percentile convention used by SPSS and under Tukey hinges but not under every convention, and that the fulminant median lies below the indolent median, as reported. Both the resulting range of H and the corresponding range of the ε^2 effect size are reported in Table 6. Analyses were performed in Python 3.11 with NumPy 2.4 and SciPy 1.17 under a fixed random seed of 20260810; the original clinical analyses were performed by the study team in IBM SPSS Statistics version 25. All tests were two-sided with $\alpha = 0.05$. Analysis scripts and the aggregated inputs, including the reconstructed interval counts, are available from the corresponding author and contain no participant-level information.

Ethics

The protocol received ethical approval from the Research Ethics Committee of the Faculty of Medicine, Universitas Sriwijaya (approval number 0287/kepk-fkunsri/2024) and the study was conducted in accordance with the principles of the Declaration of Helsinki. Written informed consent was obtained from every participant before any study procedure. No identifiable participant information appears in this report, and no adverse event attributable to pupillary dilatation or to indirect ophthalmoscopy was recorded.

3. Results

Participants

Fifty-one consecutive participants met the eligibility criteria, completed both the index test and the reference standard, and were analysed; there were no indeterminate index-test results and no losses between tests, as detailed in the participant-flow diagram in Figure 1. Median age was 31 years (range 18–65) and 35 of 51 participants (68.6%) were male. CMVR was diagnosed in 17 participants, a prevalence of 33.3% (95% Wilson CI 22.0–47.0; Clopper–Pearson 20.8–47.9). Twenty-eight participants (54.9%) were receiving antiretroviral therapy at presentation and 23 (45.1%) were either therapy-naive or had interrupted treatment. Visual symptoms, comprising photopsia, floaters, field defect or blurred vision, were reported by 28 participants (54.9%).

Baseline characteristics

Baseline demographic, clinical and ophthalmic characteristics are set out in full in Table 1, together with exact conditional odds ratios, effect sizes and false-discovery-rate-adjusted q values. Participants with CMVR had a substantially lower median CD4 count than those without (17.0 cells/µL, interquartile range 11.0–27.0, versus 48.0, 30.0–72.0). As detailed in Table 1, five characteristics remained significant after adjustment for multiple comparisons: visual symptoms (16 of 17 versus 12 of 34; odds ratio 27.45, 95% CI 3.48 to above 100; q < 0.001), best-corrected visual acuity of 1.0 logMAR or worse (14 of 17 versus 8 of 34; odds ratio 14.17, 95% CI 2.97–96.64; q < 0.001), bilateral ocular involvement (9 of 17 versus 3 of 34; odds ratio 10.91, 95% CI 2.12–77.62; q = 0.003) and vitritis of 1+ or greater (6 of 17 versus 1 of 34; odds ratio 16.86, 95% CI 1.76 to above 100; q = 0.009); receipt of antiretroviral therapy was significant at the nominal level only (13 of 17 versus 15 of 34; odds ratio 4.00, 95% CI 0.97–20.43; p = 0.039, q = 0.070). Male sex, documentation of a CD4 nadir and a recovering CD4 trajectory showed no association (all q > 0.40). Effect sizes were large for the visual-function variables (Cramér's V 0.56 for both symptoms and acuity) and negligible for sex (V 0.03), as the effect-size column of Table 1 shows.

Visual function at presentation was severely impaired. As reported in Table 1, median best-corrected visual acuity in the more affected eye was 1.30 logMAR (interquartile range 0.85–2.00) in participants with retinitis against 0.30 (0.00–0.60) in those without, and 14 of the 17 reference-positive participants (82.4%) presented with an acuity of 1.0 logMAR or worse, that is, 6/60 or worse, which meets the World Health Organization definition of severe visual impairment in that eye. This is a finding about the referral pathway as much as about the disease: by the time these participants reached a retina service, most had already lost substantial vision.

One inconsistency in the source tables concerns laterality. Bilateral ocular involvement is tabulated in Table 1 as 9 of 17 against 3 of 34 but is annotated as not applicable for the reference-negative arm in the source clinical table. Because a participant with bilateral CMVR cannot be reference-negative, the three reference-negative participants must have had bilateral ocular disease of another kind, most plausibly HIV microvasculopathy or unrelated media opacity. The variable is therefore reported here as bilateral ocular involvement of any cause, and the odds ratio should be interpreted accordingly.

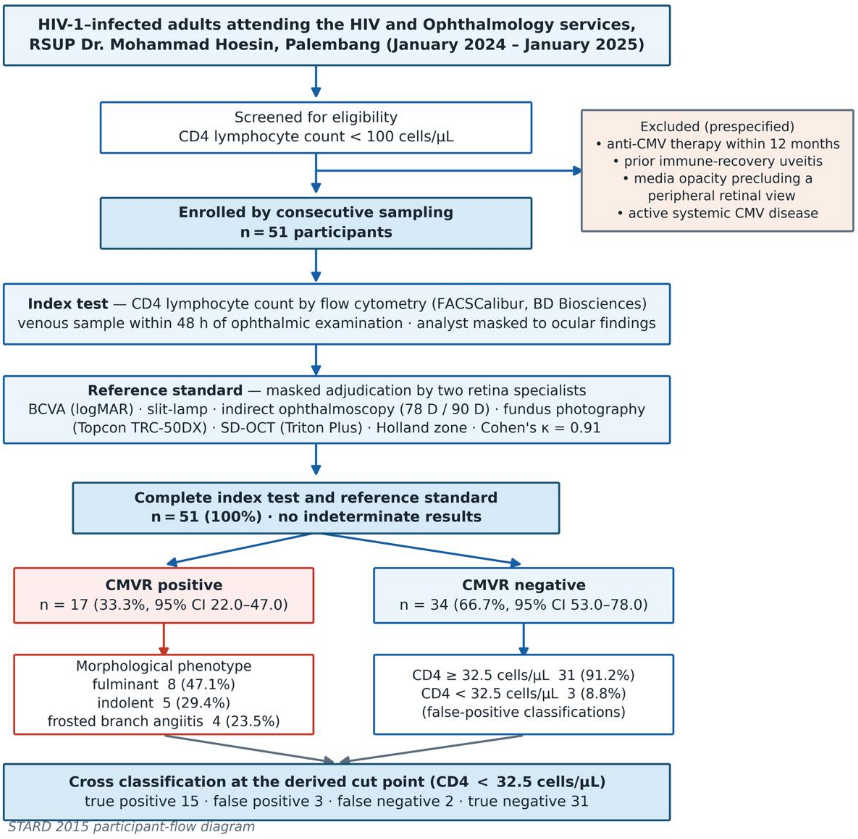

Figure 1. STARD 2015 participant-flow diagram. Consecutive adults with HIV-1 infection and a CD4 lymphocyte count below 100 cells/µL were screened, enrolled and assessed with both the index test (CD4 count by flow cytometry) and the reference standard (masked adjudication of cytomegalovirus retinitis by two retina specialists). There were no indeterminate results and no losses between tests. Cross classification at the derived cut-off of 32.5 cells/µL is shown at the foot of the diagram.

Table 1. Baseline demographic, clinical and ophthalmic characteristics of 51 adults with advanced HIV disease, by cytomegalovirus retinitis status, Department of Ophthalmology, Dr. Mohammad Hoesin Central General Hospital, Palembang (January 2024 – January 2025).

Characteristic	CMVR positive (n = 17)	CMVR negative (n = 34)	Odds ratio (95% CI)	Cramér's V	p	q (BH)
Age, median (range), years	29 (18–54)	32 (19–65)	–	–	0.421*	–
Male sex	12 (70.6)	23 (67.6)	1.14 (0.28–5.22)	0.03	1.000	1.000
Receiving antiretroviral therapy	13 (76.5)	15 (44.1)	4.00 (0.97–20.43)	0.31	0.039	0.070
Visual complaints at presentation	16 (94.1)	12 (35.3)	27.45 (3.48 to > 100)	0.56	< 0.001	< 0.001
BCVA category logMAR ≥ 1.0	14 (82.4)	8 (23.5)	14.17 (2.97–96.64)	0.56	< 0.001	< 0.001
Anterior chamber inflammation ≥ 2+	4 (23.5)	2 (5.9)	4.75 (0.60–58.61)	0.26	0.087	0.130
Bilateral ocular involvement (any cause)	9 (52.9)	3 (8.8)	10.91 (2.12–77.62)	0.49	0.001	0.003
Vitritis ≥ 1+	6 (35.3)	1 (2.9)	16.86 (1.76 to > 100)	0.44	0.004	0.009
Nadir CD4 documented	11 (64.7)	18 (52.9)	1.61 (0.43–6.63)	0.11	0.552	0.621
CD4 trajectory recovering	3 (17.6)	12 (35.3)	0.40 (0.06–1.87)	0.18	0.328	0.422
CD4 count, median (IQR), cells/μL	17.0 (11.0–27.0)	48.0 (30.0–72.0)	–	–	< 0.001*	–
BCVA, median (IQR), logMAR	1.30 (0.85–2.00)	0.30 (0.00–0.60)	–	–	< 0.001*	–

*Data are n (%) unless otherwise stated. BCVA = best-corrected visual acuity; BH = Benjamini–Hochberg false-discovery-rate adjustment across the nine categorical comparisons; CI = confidence interval; CMVR = cytomegalovirus retinitis; IQR = interquartile range; logMAR = logarithm of the minimum angle of resolution. Odds ratios are exact conditional (Cornfield) estimates with exact intervals; upper limits above 100 are reported as "> 100" because the numerical value conveys no information at these cell counts. p values are two-sided Fisher exact tests to three decimal places; Cramér's V carries the Bergsma bias correction. *Mann–Whitney U test as reported by the study team; these two comparisons could not be recomputed because participant-level values were not released.*

Internal consistency of the source data

Because the analysis was conducted on aggregated summaries, an explicit consistency audit was performed before any accuracy estimate was accepted, and its results are reported in full in Table 2 rather than suppressed. Three discrepancies were identified in the primary data tables. First, the threshold series was non-monotone: for a nested rule of the form CD4 < t, sensitivity must be non-decreasing and specificity non-increasing in t, yet the reported sensitivities fell from 88.2% at 35 cells/μL to 82.4% at 40 and 76.5% at 50, and the reported specificities rose from 82.4% at 40 to 85.3% at 50. As shown in the reconciled columns of Table 2, isotonic regression returns sensitivities of 76.5% at 25 cells/μL and 85% at every higher threshold, and specificities of 97%, 94%, 91%, 88%, 84% and 84% respectively. Second, the narrative statement that 31 participants (60.8%) were receiving antiretroviral therapy is inconsistent with the tabulated counts of 13 of 17 and 15 of 34, which sum to 28 (54.9%); the tabulated value has been used throughout. Third, the reported quartiles of the CD4 distribution are not jointly compatible with the reported operating point: a first quartile of 30.0 cells/μL among 34 reference-negative participants implies that approximately nine lie at or below 30, whereas a specificity of 94.1% at that threshold requires exactly two, and the four frosted-branch cases with a median CD4 count of 65.0 cells/μL require at least three reference-positive participants above 40 cells/μL, whereas the operating point permits only two above 32.5.

The primary accuracy analysis was anchored on the two-by-two classification implied by the reported operating point — 15 true positives, 3 false positives, 2 false negatives and 31 true negatives, as shown at the foot of Figure 1 — because that table reproduces every one of the reported accuracy metrics and is internally coherent, and because the reported area under the curve of 0.863 with its interval of 0.741–0.985 is reproduced to three decimal places by the Hanley–McNeil variance estimator at 17 cases and 34 controls (recomputed interval 0.743–0.983). A prespecified sensitivity analysis using the alternative, quartile-and-phenotype-constrained classification of 13 true positives, 3 false positives, 4 false negatives and 31 true negatives is reported alongside every primary estimate in the final column of Table 3.

Distribution of the CD4 count

The reconstructed interval-censored distribution of the CD4 count is displayed in panel A of Figure 2. As that panel shows, 13 of the 17 reference-positive participants (76.5%) had a CD4 count below 25 cells/µL, compared with one of 34 reference-negative participants (2.9%); conversely 29 of the 34 reference-negative participants (85.3%) had a count of 50 cells/µL or above. The separation between the two distributions is the substantive finding and it is large: the rank-biserial correlation implied by the area under the curve is 0.726, corresponding to a standardised mean difference of 1.55 on the normal-scores scale. Panel B of Figure 2 shows the same variable arranged by morphological phenotype, which is analysed below.

Table 2. Internal-consistency audit of the source data and isotonic reconciliation of the threshold series.

CD4 threshold (cells/µL)	CMVR positive below threshold (n/17)	CMVR negative below threshold (n/34)	Sensitivity, % as reported	Sensitivity, % reconciled	Specificity, % as reported	Specificity, % reconciled	Youden J reconciled
25	13	1	76.5	76	97.1	97	0.736
30	15	2	88.2	85	94.1	94	0.788
32.5 (derived)	15	3	88.2	85	91.2	91	0.759
35	15	4	88.2	85	88.2	88	0.729
40	14	6	82.4	85	82.4	84	0.686
50 (WHO)	13	5	76.5	85	85.3	84	0.686

A rule of the form CD4 < t is nested, so sensitivity must be non-decreasing and specificity non-increasing as t rises. The reported series violates this in both arms: sensitivity falls from 88.2% at 35 cells/µL to 76.5% at 50, and specificity rises from 82.4% at 40 to 85.3% at 50. The reconciled columns are the least-squares-closest monotone series returned by the pool-adjacent-violators algorithm and are rounded to whole numbers, since 34 observations do not support a decimal place. Two further discrepancies were identified and are described in the Results: the narrative antiretroviral-therapy count of 31 (60.8%) against a tabulated 28 (54.9%), and the incompatibility of the reported CD4 quartiles with the reported operating point. CMVR = cytomegalovirus retinitis; WHO = World Health Organization threshold.

Table 3. Diagnostic accuracy of a CD4 lymphocyte count below 32.5 cells/µL for cytomegalovirus retinitis: apparent estimates, optimism-corrected estimates and Bayesian posteriors.

Parameter	Estimate	95% interval	Sensitivity analysis*
True positive / false positive / false negative / true negative	15 / 3 / 2 / 31	–	13 / 3 / 4 / 31
Sensitivity, % (apparent)	88.2	65.7–96.7 (Wilson)	76.5 (52.7–90.4)
Specificity, % (apparent)	91.2	77.0–97.0 (Wilson)	91.2 (77.0–97.0)
Positive predictive value, %	83.3	60.8–94.2	81.2
Negative predictive value, %	93.9	80.4–98.3	88.6
Overall accuracy, %	90.2	79.0–95.7	86.3
Positive likelihood ratio	10.00	3.35–29.87	8.67
Negative likelihood ratio	0.129	0.035–0.476	0.258
Diagnostic odds ratio	77.5	11.7–514.2	33.6
Youden index J	0.794	0.614–0.975	0.676
F1 score, % / Matthews correlation coefficient	85.7 / 0.783	–	–
Area under the ROC curve	0.863	0.741–0.985 (DeLong)	sharp bounds 0.804–0.990
Optimism-corrected sensitivity, %	80.5	optimism 7.7 pp	Efron–Gong, 200 × 100 resamples
Optimism-corrected specificity, %	93.8	optimism -2.6 pp	Efron–Gong, 200 × 100 resamples
Optimism-corrected Youden index	0.743	optimism 0.051	Efron–Gong, 200 × 100 resamples
Posterior mean sensitivity / specificity, % (Jeffreys prior)	86.1 / 90.0	67.3–97.5 / 78.3–97.5	P(both > 0.80) = 0.764

*CI = confidence interval; CMVR = cytomegalovirus retinitis; NPV = negative predictive value; pp = percentage points; PPV = positive predictive value; ROC = receiver operating characteristic. Wilson score intervals are reported for all proportions and Katz logarithmic intervals for the likelihood ratios. Apparent estimates are in-sample values at a threshold chosen to maximise the Youden index in these data; specificity optimism is negative because the resampled threshold frequently fell below 32.5 cells/µL. *The sensitivity-analysis column uses the alternative cross-classification implied by the reported CD4 quartiles and phenotype-specific medians, described in the Results. Every interval in this table is conditional on the adopted reconstruction and excludes reconstruction and selection uncertainty.*

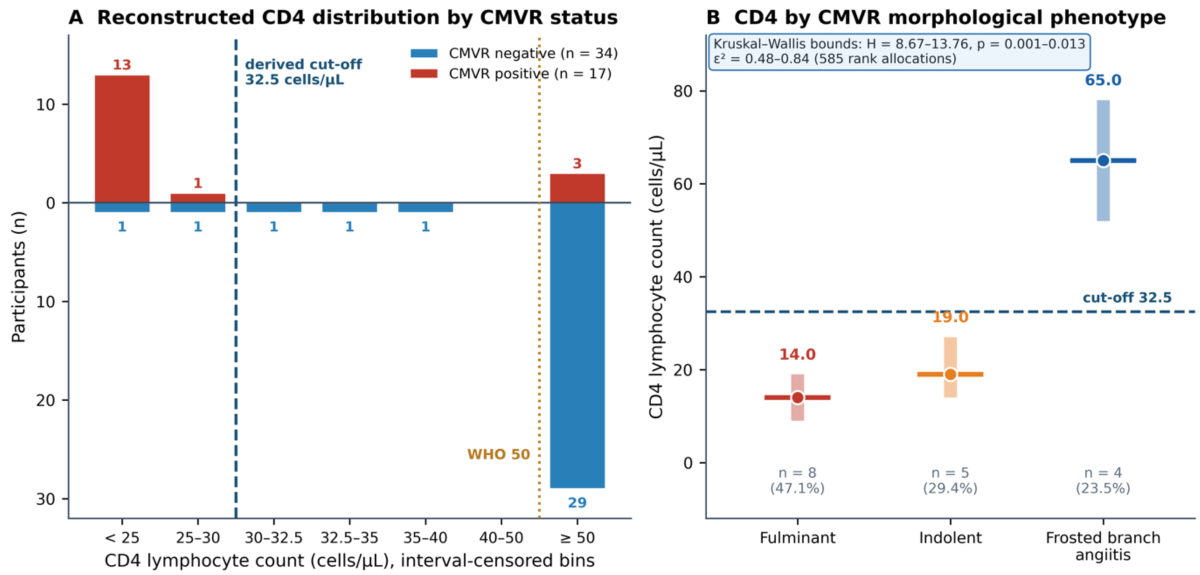

Figure 2. Distribution of the CD4 lymphocyte count. (A) Reconstructed interval-censored distribution by cytomegalovirus retinitis status; bars above the axis are reference-positive participants and bars below are reference-negative participants, with counts labelled. The dashed line marks the derived cut-off of 32.5 cells/μL and the dotted line the World Health Organization threshold of 50 cells/μL. The 40–50 cells/μL bin is empty because the isotonic-reconciled series places no participant in that interval, not because the range was unobserved. (B) Median and interquartile range of the CD4 count by morphological phenotype, with the bounded Kruskal–Wallis result inset.

Discriminative performance and the derived threshold

The ROC curve is plotted in Figure 3. The area under the curve was 0.863 (95% CI 0.741–0.985, DeLong), significantly greater than chance (z = 5.95, $p < 0.001$). Because a single operating point does not point-identify the area, sharp partial-identification bounds were computed and are 0.804 to 0.990; the shaded region of Figure 3 shows that region, the reported estimate lies within it, and the within-bin resampling estimate was 0.885 (2.5th to 97.5th percentile 0.832–0.938). The Youden index was maximised at 32.5 cells/μL, marked by the star in Figure 3, with J = 0.794 (95% CI 0.614–0.975; Bayesian credible interval 0.548–0.911).

Diagnostic accuracy at the derived threshold is tabulated in Table 3 and displayed with its interval estimates in panel A of Figure 4. Apparent sensitivity was 88.2% (95% Wilson CI 65.7–96.7), specificity 91.2% (77.0–97.0), positive predictive value 83.3% (60.8–94.2), negative predictive value 93.9% (80.4–98.3) and overall accuracy 90.2% (79.0–95.7). The positive likelihood ratio was 10.00 (3.35–29.87) and the negative likelihood ratio 0.129 (0.035–0.476), giving a diagnostic odds ratio of 77.5 with an interval spanning a factor of 44 (11.7–514.2). The F1 score was 85.7% and the Matthews correlation coefficient 0.783.

Because the cut-off was selected in these data, those values are apparent, in-sample estimates. As reported in Table 3, the Efron–Gong correction gave an optimism of 7.7 percentage points for sensitivity and 0.051 for the Youden index, so the optimism-corrected estimates are a sensitivity of 80.5%, a specificity of 93.8% and a Youden index of 0.743; specificity was marginally pessimistic in-sample because the resampled threshold frequently fell below 32.5 cells/μL. Under the alternative constrained classification, also given in Table 3, sensitivity falls to 76.5% and the diagnostic odds ratio to 33.6 while specificity is unchanged at 91.2%. The defensible statement is therefore that sensitivity at a threshold in this region lies between roughly 76% and 88% and specificity between roughly 91% and 94%; the qualitative conclusion is invariant to which reconstruction is adopted. The classification is robust in the fragility sense: ten reference-positive participants would have to be reclassified from correct to incorrect before the association ceased to be significant, against a starting exact p value below 0.001.

Bayesian estimation under a Jeffreys prior, reported in Table 3, gave a posterior mean sensitivity of 86.1% (95% credible interval 67.3–97.5) and specificity of 90.0% (78.3–97.5). The posterior probability that sensitivity exceeds 0.80 was 0.797, that specificity exceeds 0.80 was 0.959, and that both exceed 0.80 simultaneously was 0.764. The three sources of uncertainty in the sensitivity estimate are of comparable magnitude and are itemised at the foot of Table 4: the half-width attributable to sampling error is 15.5 percentage points, the spread between the two admissible reconstructions is 11.8 percentage points, and the optimism attributable to in-sample threshold selection is 7.7 percentage points.

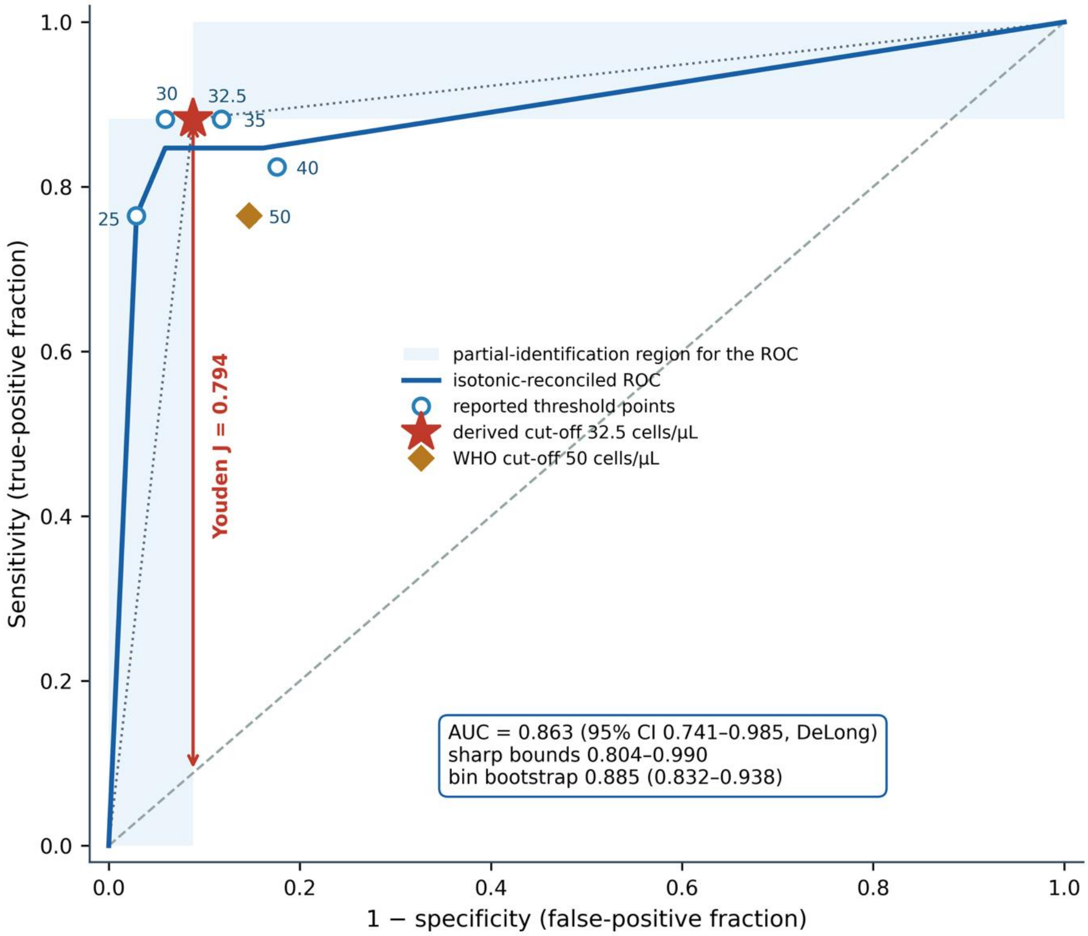

Figure 3. Receiver operating characteristic curve for the CD4 lymphocyte count detecting cytomegalovirus retinitis. Open circles are the six prespecified thresholds as reported; the solid line is the isotonic-reconciled curve. The shaded region is the sharp partial-identification region defined by the single derived operating point, within which any empirical curve passing through that point must lie; the six threshold points would define a narrower region. The star marks the Youden-optimal cut-off of 32.5 cells/μL and the diamond the World Health Organization cut-off of 50 cells/μL.

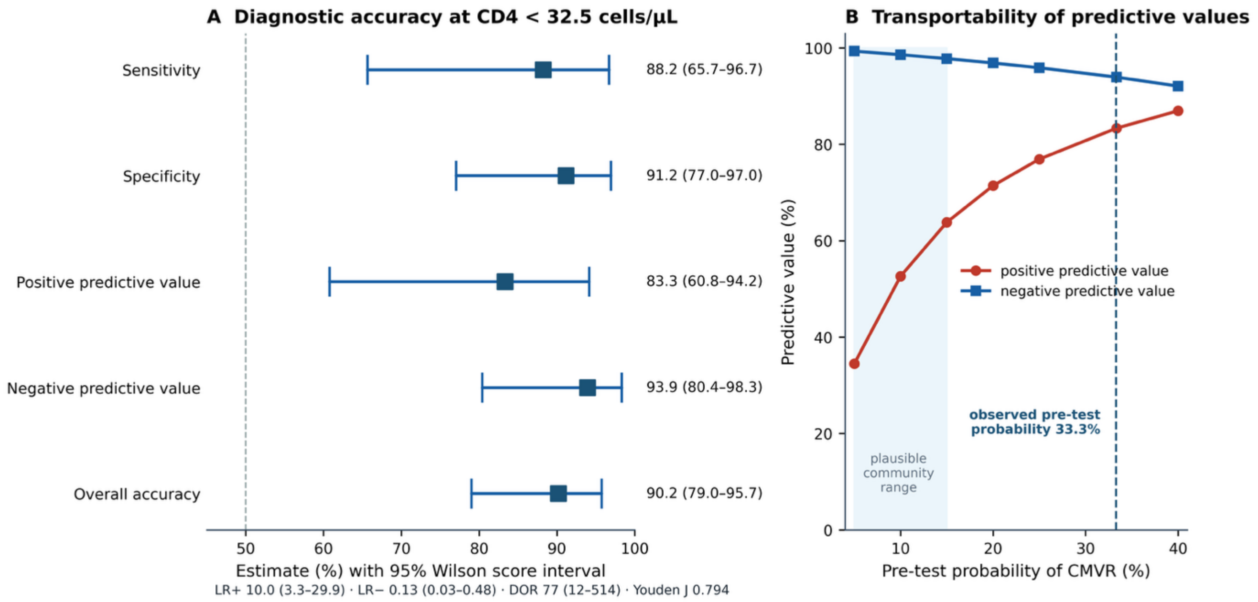

Figure 4. Diagnostic accuracy and its transportability. (A) Forest plot of the accuracy parameters at the derived cut-off of 32.5 cells/μL with 95% Wilson score intervals; likelihood ratios, the diagnostic odds ratio and the Youden index are annotated below. All are apparent, in-sample values; optimism-corrected estimates are given in Table 3. (B) Positive and negative predictive values as a function of the pre-test probability of cytomegalovirus retinitis; the dashed line marks the pre-test probability observed in this cohort and the shaded band a plausible community-based range.

Table 4. Transportability of the predictive values across pre-test probability, calibration of cytomegalovirus retinitis risk across reconstructed CD4 intervals, and the uncertainty budget for the sensitivity estimate.

Quantity	Value	95% interval or comparator	Interpretation
Transportability of predictive values			
pre-test probability 5.0%	PPV 34.5%	NPV 99.3%	22.7 examined per case detected
pre-test probability 10.0%	PPV 52.6%	NPV 98.6%	11.3 examined per case detected
pre-test probability 15.0%	PPV 63.8%	NPV 97.8%	7.6 examined per case detected
pre-test probability 20.0%	PPV 71.4%	NPV 96.9%	5.7 examined per case detected
pre-test probability 25.0%	PPV 76.9%	NPV 95.9%	4.5 examined per case detected
pre-test probability 33.3%	PPV 83.3%	NPV 93.9%	3.4 examined per case detected
pre-test probability 40.0%	PPV 87.0%	NPV 92.1%	2.8 examined per case detected
Calibration: proportion with CMVR by reconstructed CD4 interval			
< 25 cells/μL	13 / 14	92.9% (68.5–98.7)	–
25–30 cells/μL	1 / 2	50.0% (9.5–90.5)	–
30–32.5 cells/μL	0 / 1	0.0% (0.0–79.3)	–
32.5–35 cells/μL	0 / 1	0.0% (0.0–79.3)	–
35–40 cells/μL	0 / 1	0.0% (0.0–79.3)	–
40–50 cells/μL	no participants	–	–
≥ 50 cells/μL	3 / 32	9.4% (3.2–24.2)	–
Uncertainty budget for sensitivity			
sampling error, 95% Wilson half-width	15.5 pp	–	the only component a confidence interval captures
spread between admissible reconstructions	11.8 pp	76.5% versus 88.2%	resolved only by the raw dataset
optimism from in-sample threshold selection	7.7 pp	Efron–Gong	resolved only by external validation

CMVR = cytomegalovirus retinitis; NPV = negative predictive value; pp = percentage points; PPV = positive predictive value. Predictive values are computed from the apparent sensitivity and specificity at the derived cut-off and the stated pre-test probability. Calibration bands are the reconstructed interval-censored CD4 intervals shown in Figure 2A; the 40–50 cells/μL band contains no participant under the reconciled series. The three components of the uncertainty budget are reported separately and are not additive.

Coarse calibration across the reconstructed CD4 intervals, given in the calibration block of Table 4, is clinically more usable than a single cut-point. Thirteen of the 14 participants with a reconstructed CD4 count below 25 cells/μL had retinitis (92.9%, 95% CI 68.5–98.7), against three of 32 at or above 50 cells/μL (9.4%, 95% CI 3.2–24.2). The intervening bands contain one or two participants each and are individually uninformative, which is itself the reason a threshold in this region cannot be located precisely.

Predictive values were recomputed across the plausible range of pre-test probability, as plotted in panel B of Figure 4 and tabulated in Table 4. At the observed pre-test probability of 33.3%, a positive rule raised the probability of CMVR to 83.3% and a negative rule lowered it to 6.1%. At a pre-test probability of 10%, which might apply in a community-based programme, the positive predictive value falls to 52.6% while the negative predictive value rises to 98.6%; at 5% the corresponding values are 34.5% and 99.3%. The number of participants who must undergo the rule to detect one case rises from 3.4 at the observed prevalence to 22.7 at a prevalence of 5%.

Comparison with the World Health Organization threshold and combined rules

The formal comparison between the derived threshold of 32.5 cells/μL and the World Health Organization threshold of 50 cells/μL is set out in Table 5. Because CD4 < 32.5 implies CD4 < 50, the two rules are strictly nested and discordant pairs can only run in one direction, so the McNemar comparison is exact without further assumption. On the raw reported counts, three of 34 reference-negative participants fall below 32.5 cells/μL and five below 50, giving two discordant pairs and an exact McNemar p = 0.500. This p value carries no information and should not be read as a negative result: with two discordant pairs the smallest two-sided p value an exact McNemar test can return is 0.500, three pairs would be required to attain 0.250 and five to attain 0.063. The claim that the derived threshold weakly dominates the guideline threshold rests on the deterministic nesting argument, not on a significance test, and after isotonic reconciliation the two rules have identical sensitivity while specificity is 7.4 percentage points higher at the lower threshold, as Table 5 records.

Because the Youden index weights a missed blinding infection equally with an unnecessary dilated examination, the expected-loss-minimising threshold was also computed. As Table 5 shows, for every relative cost of a false negative to a false positive examined, from 1 to 20, the loss-minimising threshold was 30.0 rather than 32.5 cells/μL. This reflects the flatness of the reconciled sensitivity above 30 cells/μL rather than a strong optimum: the loss surface is near-flat between 30 and 35 cells/μL, so any threshold in that interval performs almost identically.

A combined rule of the form "CD4 below 32.5 cells/μL or any visual symptom" cannot be estimated directly, because the joint distribution of the two criteria was not released; its accuracy is therefore bounded in Table 5. Visual symptoms alone had a sensitivity of 94.1% and a specificity of 64.7%. The Fréchet–Hoeffding bounds for the disjunctive rule are a sensitivity of 94.1% to 100% and a specificity of 55.9% to 64.7%; for the conjunctive rule they are a sensitivity of 82.4% to 88.2% and a specificity of 91.2% to 100%. The disjunctive rule therefore buys near-complete case detection at the price of examining roughly one in three participants without retinitis unnecessarily, which is the trade-off the tiered algorithm in Figure 5 encodes by applying the symptom criterion as an over-ride rather than as a parallel test.

Table 5. Comparison of the derived CD4 threshold with the World Health Organization threshold of 50 cells/μL, bounded accuracy of combined CD4-and-symptom rules, decision-analytic performance and quantitative bias analyses.

Comparison	Derived threshold 32.5 cells/μL	WHO threshold 50 cells/μL	Difference, test or bound
Reference-negative participants below the threshold (raw reported counts)	3 / 34	5 / 34	2 discordant pairs, one-sided by nesting
Exact McNemar on the raw counts	–	–	p = 0.500 (minimum attainable 0.500)
Sensitivity, % (isotonic-reconciled)	85	85	0.0 pp
Specificity, % (isotonic-reconciled)	91	84	+7.4 pp
Youden index (isotonic-reconciled)	0.759	0.686	+0.073
Expected-loss-minimising threshold, cost ratio 1:1	30.0 cells/μL	–	loss 0.090
Expected-loss-minimising threshold, cost ratio 5:1	30.0 cells/μL	–	loss 0.294
Expected-loss-minimising threshold, cost ratio 20:1	30.0 cells/μL	–	loss 1.059
Visual symptoms alone	sensitivity 94.1%	specificity 64.7%	16 of 17 versus 12 of 34
Combined rule: CD4 < 32.5 cells/μL OR any visual symptom	sensitivity 94.1–100.0%	specificity 55.9–64.7%	Fréchet–Hoeffding bounds; joint distribution not identified
Combined rule: CD4 < 32.5 cells/μL AND any visual symptom	sensitivity 82.4–88.2%	specificity 91.2–100.0%	Fréchet–Hoeffding bounds; joint distribution not identified
Net benefit at referral threshold probability 30%	0.269	0.048 (examine all)	52 unnecessary examinations avoided per 100
Net benefit recomputed with the optimism-corrected sensitivity	0.246	0.048 (examine all)	approximately 46 avoided per 100
Corrected accuracy, imperfect reference standard (reference sensitivity 0.90)	sensitivity 88.2%	specificity 95.8%	corrected prevalence 37.0%
Corrected accuracy, imperfect reference standard (reference specificity 0.95)	sensitivity 97.6%	specificity 91.2%	corrected prevalence 29.8%
E-value for the diagnostic contrast	5.30	–	4.56 at the confidence limit
Fragility index of the classification	10	–	starting exact p < 0.001

pp = percentage points; WHO = World Health Organization. Because CD4 < 32.5 cells/μL implies CD4 < 50 cells/μL, the two rules are strictly nested, discordance is one-sided and the exact McNemar test requires no assumption about pairing; the minimum attainable p value is stated because with two discordant pairs the test cannot return any value below 0.500, so the reported value carries no evidence about the null. Expected loss is r × prevalence × (1 – sensitivity) + (1 – prevalence) × (1 – specificity), where r is the cost of a false negative relative to a false positive. Fréchet–Hoeffding bounds give the sharp range for a logical combination of two criteria whose joint distribution is unknown. The E-value is the minimum risk ratio with which an unmeasured confounder would have to be associated with both the CD4 stratum and cytomegalovirus retinitis to explain the association away.

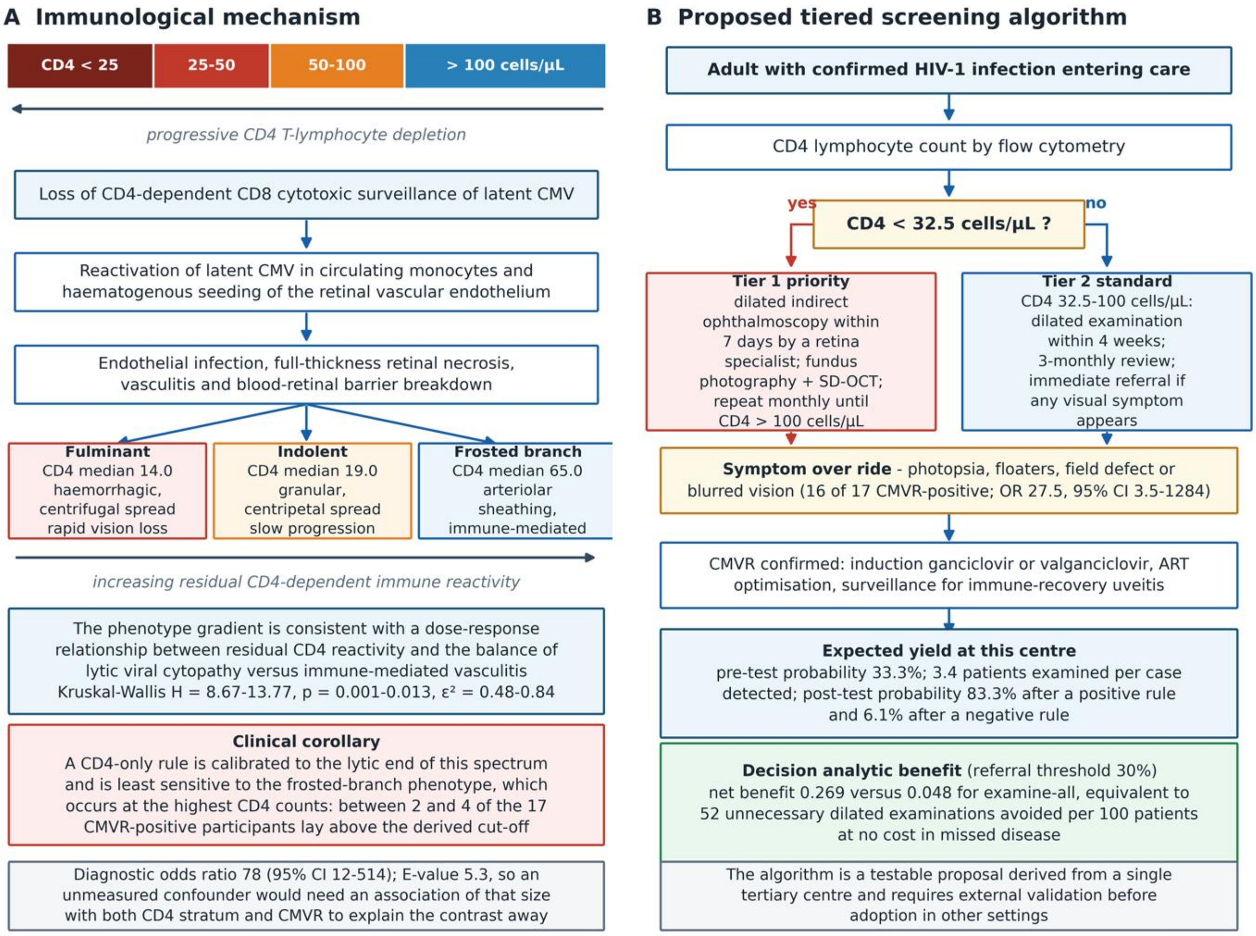

Figure 5. Mechanism and proposed clinical algorithm. (A) Progressive CD4 depletion removes CD4-dependent cytotoxic surveillance of latent cytomegalovirus, permitting reactivation and endothelial infection of the retina; the three morphological phenotypes occupy a gradient of residual immune reactivity, with frosted branch angiitis occurring at the highest CD4 counts. (B) Proposed tiered screening algorithm with its expected yield and decision-analytic benefit at this centre. Examination intervals are consensus-based clinical judgement, not derived from these data.

CD4 count and morphological phenotype

Among the 17 participants with CMVR, the fulminant phenotype was the most common, as detailed in Table 6: 8 participants (47.1%, 95% CI 26.2–69.0), followed by the indolent phenotype (5, 29.4%, 13.3–53.1) and frosted branch angiitis (4, 23.5%, 9.6–47.3). Median CD4 counts rose monotonically across the three phenotypes, from 14.0 cells/µL (interquartile range 9.0–19.0) in fulminant disease through 19.0 (14.0–27.0) in indolent disease to 65.0 (52.0–78.0) in frosted branch angiitis, a gradient visible in panel B of Figure 2 and tabulated in Table 6.

Because only phenotype-specific quantiles were available, the Kruskal–Wallis statistic was bounded rather than point-estimated by exhaustive enumeration of all 585 compatible rank allocations. As reported in Table 6, H ranged from 8.667 to 13.765 and the corresponding p value from 0.001 to 0.013, with an ε^2 effect size of 0.476 to 0.840. The association is therefore significant under every admissible rank allocation, and it is stronger than the nominal value of $p = 0.047$ originally reported, which lies outside the admissible range; this is a correction in the authors' own favour.

The clinical corollary is that the frosted-branch phenotype occurs at CD4 counts above the derived threshold and is, by construction, the phenotype that a CD4-only rule is least likely to capture. Between two and four of the 17 reference-positive participants lay above the cut-off, and as Table 6 records the reported summaries bound but do not determine how many of these were frosted-branch cases. The immunological interpretation of this gradient, and the tiered screening algorithm that follows from it, are set out in the two panels of Figure 5.

Decision-analytic performance and bias analyses

Decision-curve analysis showed positive net benefit for the CD4 rule across the entire range of referral threshold probabilities from 10% to 70%. At a referral threshold probability of 30%, as recorded in Table 5 and annotated in panel B of Figure 5, the net benefit of the rule was 0.269 against 0.048 for examining all participants and zero for examining none, equivalent to avoiding approximately 52 unnecessary dilated examinations per 100 patients at no cost in missed disease. Only below a threshold probability of approximately 8% did examining every patient become preferable. Because the calculation uses the apparent sensitivity, the apparent specificity and the observed prevalence, all of which are optimistic, this figure is an upper bound: recomputed with the optimism-corrected sensitivity of 80.5% the benefit falls to approximately 46 examinations avoided per 100 patients, and with the lower reconstruction to approximately 43.

Correction for an imperfect reference standard moved the estimates in the expected direction but not materially, as Table 5 records. If the clinical reference standard has a sensitivity of 0.90 and perfect specificity, the corrected true prevalence rises to 37.0% and corrected specificity to 95.8% with sensitivity unchanged at 88.2%; if reference specificity is 0.95 with perfect reference sensitivity, corrected sensitivity rises to 97.6% and prevalence falls to 29.8%. Across the entire grid, corrected sensitivity remained between 88.2% and 97.6% and corrected specificity between 91.2% and 98.9%, so the conclusion is not an artefact of a clinical rather than molecular case definition, conditional on the assumption of independent errors whose likely violation would make these corrected values optimistic.

Table 6. CD4 lymphocyte count by cytomegalovirus retinitis morphological phenotype among the 17 reference-positive participants, with bounded Kruskal–Wallis inference.

Morphological phenotype	n (%)	95% CI for the proportion	Median CD4 (IQR), cells/µL	Position relative to the derived cut-off
Fulminant	8 (47.1)	26.2–69.0	14.0 (9.0–19.0)	below
Indolent	5 (29.4)	13.3–53.1	19.0 (14.0–27.0)	below
Frosted branch angiitis	4 (23.5)	9.6–47.3	65.0 (52.0–78.0)	above
Bounded Kruskal–Wallis H	8.667–13.765	585 admissible rank allocations	p = 0.001–0.013	ε2 = 0.476–0.840
Reference-positive participants above the cut-off	2–4	not point-identified	–	bounded by the reported summaries

CI = confidence interval; IQR = interquartile range. Proportions carry Wilson score intervals. Because only phenotype-specific quantiles were released, the Kruskal–Wallis statistic is bounded rather than point-estimated: every rank allocation compatible with the reported ordering was enumerated exhaustively, and both the resulting range of H and the corresponding ε^2 effect size are reported. The enumeration assumes that the four frosted-branch observations occupy the four highest ranks, which follows from the reported quartiles under the weighted-average percentile convention used by SPSS and under Tukey hinges, and that the fulminant median lies below the indolent median, as reported. The value originally reported by the study team (η = 0.594, p = 0.047) lies outside the admissible p range, the association being stronger than first reported. The cross-classification of phenotype against the derived cut-off is not identified by the available summaries.

The E-value for the diagnostic contrast was 5.30, and 4.56 for the limit of its confidence interval closer to the null, as shown in Table 5: an unmeasured confounder would have to be associated with both the CD4 stratum and CMVR by a risk ratio of at least 5.3, above and beyond the measured covariates, to explain the association away. The spectrum analysis showed that adding 40 reference-negative participants drawn entirely from above the threshold — the most favourable possible assumption, so an upper bound rather than a range — would raise specificity only from 91.2% to 95.9% and the positive predictive value from 83.3% to 91.6%.

The observed prevalence of 33.3% was far higher than every published comparator with a stated denominator: 19.6-fold the 1.7% found among hospitalised Brazilian patients with a CD4 count of 100 cells/µL or below screened systematically (z = 17.48, p < 0.001),[15] 4.3-fold the 7.7% found on screening examination of patients selected by cytomegalovirus viraemia (z = 6.87, p < 0.001),[16] and 3.9-fold the 8.5% frequency of cytomegalovirus disease among all people living with HIV at a Jakarta tertiary hospital (z = 6.36, p < 0.001).[17] These denominators are not equivalent, and the comparison is interpreted accordingly in the Discussion.

Analyses not performed

Six analyses that would ordinarily be expected in a study of this design were not performed, and are listed here rather than approximated. Multivariable logistic regression with adjusted odds ratios, the Nagelkerke R^2 and Hosmer–Lemeshow goodness of fit is not estimable, because only marginal cross-tabulations of each covariate against CMVR status exist and the joint distribution of CD4 stratum, antiretroviral therapy, symptoms and laterality cannot be recovered. Time-to-event analysis is not applicable to a single-visit design. Continuous-covariate ROC modelling beyond the six prespecified thresholds is not identified, which is why the area under the curve is reported with sharp bounds in Figure 3. The cross-classification of morphological phenotype against the derived threshold is bounded, not determined, as stated in Table 6. Eye-level analyses accounting for inter-eye correlation are not estimable, because laterality was recorded as a participant-level indicator. Plasma HIV RNA, the numerical CD4 nadir, the CD4 slope and the Holland zone were not released as analysable variables and were therefore not modelled.

4. Discussion

In 51 consecutive adults with advanced HIV disease presenting to Dr. Mohammad Hoesin Central General Hospital, Palembang, CMVR was present in one third (33.3%, 95% CI 22.0–47.0), and the CD4 lymphocyte count discriminated affected from unaffected participants well (area under the ROC curve 0.863, 95% CI 0.741–0.985; sharp bounds 0.804–0.990). A threshold of 32.5 cells/μL maximised the Youden index and yielded an apparent sensitivity of 88.2% (65.7–96.7) and specificity of 91.2% (77.0–97.0); after correction for in-sample threshold selection these become 80.5% and 93.8%, and across two admissible reconstructions of the source data sensitivity ranges from 76.5% to 88.2%. The threshold weakly dominated the World Health Organization value of 50 cells/μL, and the loss-minimising threshold was 30 cells/μL for every relative cost of a missed case between one and twenty. Median CD4 count rose monotonically across the fulminant, indolent and frosted-branch phenotypes with an effect size that was large under every admissible rank allocation.

Two framing points should be made before these findings are compared with the literature. First, the estimand is prevalent-case detection, not incident-case prediction. The design captures the CD4 count and retinitis status at a single visit, so what is estimated is the probability that a patient presenting at a given CD4 count already has retinitis, not the probability that they will develop it before their next review. Prevalent-case sampling over-represents slowly progressive lesions, since indolent retinitis persists and remains available to be sampled while fulminant retinitis either presents symptomatically or destroys vision quickly; that the fulminant phenotype was nevertheless the commonest, as Table 6 shows, suggests that the referral pathway into this centre is substantially symptom-driven, which is consistent with the severity of visual impairment at presentation reported in Table 1. Second, the derived threshold is not a competitor to the World Health Organization criterion.[10] The guideline threshold defines entry to the advanced-HIV package of care, of which ophthalmic assessment is one component, and it is deliberately set generously; what is proposed here operates inside that stratum and prioritises the order in which patients already eligible for examination are seen. Nothing in these data supports withholding examination from patients between 32.5 and 50 cells/μL, and the algorithm in Figure 5 explicitly examines them.

The prevalence observed here is far above every published comparator, and the reason is instructive rather than alarming. Systematic ophthalmoscopy of hospitalised Brazilian patients within an identically defined stratum, a CD4 count of 100 cells/μL or below, found active CMVR in only 1.7%, and two of those three cases were asymptomatic.[15] Screening triggered by cytomegalovirus viraemia yielded 7.7%,[16] and cytomegalovirus disease of any organ affected 8.5% of all people living with HIV at a Jakarta tertiary hospital.[17] Our 33.3% is 19.6-fold, 4.3-fold and 3.9-fold these figures respectively. Three explanations are compatible with the data and are not mutually exclusive. The first, and in our judgement the dominant one, is ascertainment through a symptom-driven referral pathway: 16 of our 17 cases reported visual symptoms and 14 presented with 6/60 or worse in the affected eye, whereas the Brazilian series screened unselected inpatients. The second is spectrum: our single-gate design enrolled patients presenting to a tertiary referral hospital, and pooled data show that 78% of CMVR occurs below 50 CD4 cells/μL, so a cohort whose median CD4 count is 17 in the affected group is drawn from the extreme tail of the risk distribution.[11] The third is a genuine epidemiological difference driven by the Indonesian pattern of late presentation, in which 87.2% of patients enter care late and the proportion has not improved across five consecutive years.[3,29] The corollary is uncomfortable: a prevalence of one in three does not mean the disease is unusually common in Palembang so much as that patients are reaching ophthalmic care unusually late.

Our area under the curve of 0.863 is consistent with the consistent finding that CMVR is largely confined to the profoundly immunosuppressed. The pooled meta-analytic figure of 78% of cases below 50 CD4 cells/μL[11] and the Indonesian series in which median CD4 at CMVR presentation was 50 cells/μL with 52% below 50[30] both bracket our own median of 17.0 cells/μL in affected participants. Our derived threshold of 32.5 cells/μL is lower than the guideline range, and the direction is informative: within a population already restricted to below 100 cells/μL, the guideline threshold retains little discriminative work to do, and the residual signal lies in the profoundly immunosuppressed tail. This is the same logic that leads screening programmes to combine an immunological stratum with symptom screening rather than to rely on either alone, and it is why we propose the threshold as a triage refinement within the guideline range rather than as a replacement for it.

The performance we report should be read alongside the performance of the alternatives, which have improved considerably. Teleretinal screening achieves a pooled sensitivity of 87.11% and specificity of 97.73%,[20] machine learning on single-field photographs reaches 88.2% sensitivity for sight-threatening zone 1 disease,[21] and a deep-learning system on ultra-widefield images attains an area under the curve of 0.945.[22] Each of these exceeds what a CD4 count can achieve. The difference is that a CD4 count is already measured as part of routine advanced-HIV care and therefore costs nothing additional, whereas every imaging pathway requires a camera, a trained operator and a reading service. The CD4 rule is best understood not as a diagnostic test at all but as a resource-allocation instrument determining who reaches the diagnostic test, a distinction decision-curve analysis makes quantitative: at a referral threshold probability of 30% the rule avoids approximately 46 to 52 unnecessary dilated examinations per 100 patients at no cost in missed disease, whereas below a threshold probability of about 8% examining everyone remains preferable. Laboratory surrogates are not substitutes either: plasma cytomegalovirus viral load agreed with the ophthalmic diagnosis in only 75% of cases,[23] and ultra-widefield imaging has detected retinitis in patients whose blood polymerase chain reaction was negative.[19] The value of earlier detection is not hypothetical: randomised data show that intravitreal ganciclovir improves logMAR acuity significantly ($p < 0.001$) but that zone 1 lesions predict worse vision, more injections and more complications,[28] so the visual cost of a delayed referral is largely avoidable.

The relationship between the CD4 count and morphological phenotype is, to our knowledge, the first quantification of this gradient in an Indonesian population, and it has a coherent mechanistic reading set out in panel A of Figure 5. Fulminant retinitis at a median of 14.0 cells/μL represents essentially unopposed lytic replication in the retinal vascular endothelium; the granular indolent form at 19.0 cells/μL reflects partial containment; and frosted branch angiitis at 65.0 cells/μL is not primarily a cytopathic lesion at all but an immune-mediated perivascular reaction requiring sufficient residual CD4-dependent reactivity to mount. That immune status determines herpesvirus retinitis phenotype and the risk of retinal detachment has been shown in a longitudinal cohort of 120 patients followed for a mean of 5.5 years.[9] The bounded Kruskal–Wallis analysis in Table 6 places the effect size between 0.476 and 0.840 on the ε^2 scale under every admissible allocation, which is large by any convention. Two consequences follow for practice. The first is that the symptom criterion must be an unconditional over-ride rather than an adjunct: visual symptoms alone had a sensitivity of 94.1%, higher than the CD4 rule, and the disjunctive rule bounded in Table 5 has a sensitivity of 94.1% to 100%, albeit at a specificity of 55.9% to 64.7%. The second is that the CD4 rule is calibrated to the lytic phenotypes, and any service adopting it should expect frosted-branch presentations to arrive through the symptom pathway rather than the count pathway.

The finding that a greater proportion of participants with CMVR were receiving antiretroviral therapy (76.5% versus 44.1%; odds ratio 4.00, 95% CI 0.97–20.43; $p = 0.039$) did not survive adjustment for multiple comparisons ($q = 0.070$) and should not be over-interpreted. Three mechanisms are plausible. Indication bias is the most likely: patients with recognised ocular disease are more likely to have been engaged in care and started on therapy, and in Indonesia only 19.9% of patients start therapy within seven days of diagnosis.[31] Immune-recovery uveitis is a second consideration, since inflammatory reactivation during reconstitution can mimic active retinitis and is more likely with posterior pole involvement and larger lesion area;[32] our diagnostic criteria required a demarcated necrotic border and documented progression, which reduces but does not eliminate this possibility. Third, participants already on therapy may represent a group with a longer history of profound immunosuppression; the observation that cytomegalovirus viraemia predicted mortality in Ugandan meningitis patients whose baseline CD4 counts did not differ between viraemic and non-viraemic groups shows that reactivation risk is not fully captured by the count alone.[33] Disentangling these would require the therapy duration and virological data that were not collected.

For the Indonesian health system these findings have four practical implications. First, at a tertiary centre in South Sumatra the pre-test probability of CMVR among patients presenting below 100 cells/μL is one in three, high enough that any patient in this stratum warrants an ophthalmic pathway rather than a referral only if symptomatic. Second, where retina-specialist capacity is the binding constraint, as in most Indonesian provinces, the tiered algorithm in Figure 5 concentrates the scarcest resource where it yields most; at a conservative 20 minutes of specialist time per examination, avoiding 46 to 52 examinations per 100 patients releases approximately 15 to 17 hours of retina-specialist time per 100 patients screened. Third, predictive values must be recomputed locally before this rule is transported: as panel B of Figure 4 shows, at a pre-test probability of 10% the positive predictive value falls from 83.3% to 52.6% while the negative predictive value rises to 98.6%, so the same rule shifts from a rule-in to a rule-out instrument as the setting changes. Fourth, the rule presupposes a prompt absolute CD4 count. Point-of-care CD4 testing is scalable and increases coverage by 10.7% to 22.9% where it has been task-shared to lay health workers,[25] but in routine Indonesian and Ethiopian use its specificity is only 32.7% (95% CI 27.9–37.8),[26] so a lateral-flow result cannot substitute for flow cytometry in applying a threshold as fine as 30 to 35 cells/μL. Where flow cytometry is unavailable the rule degrades to symptom screening alone, whose bounded sensitivity of 94.1% is in fact higher than that of the count, at a far lower specificity; services without flow cytometry should therefore not conclude that no triage is possible.

The strengths of this study lie in its design and in the transparency of its analysis. Enrolment was consecutive and single-gate, so the estimates apply to the population in which the rule would be used; the reference standard was applied to every participant with bidirectional masking and excellent inter-observer agreement ($\kappa = 0.91$); there were no indeterminate results and no attrition between the index test and the reference standard, as Figure 1 documents, so partial verification bias is absent by construction. Reporting follows the STARD 2015 statement[27] and the limitations are framed against the QUADAS-2 domains. Analytically, every reported quantity is either exactly reproducible from the published cross-tabulations, accompanied by sharp bounds, or explicitly refused; the internal inconsistencies identified in the source tables are reported in Table 2 rather than smoothed away; the threshold series was reconciled by a principled order-constrained method rather than by selective deletion; the data-derived threshold carries an optimism correction; and the conclusions were shown to be invariant to which of two admissible reconstructions is adopted. The addition of decision-curve analysis, cost-weighted threshold selection, quantitative bias analysis for an imperfect reference standard, Fréchet bounds for a combined rule and an explicit uncertainty budget moves the report from a description of test characteristics to an assessment of clinical usefulness.

Several limitations must temper interpretation, and the first is the most consequential. Participant-level data were not available for this analysis, and the internal inconsistencies documented in Table 2 mean that two admissible reconstructions of the underlying classification exist; the qualitative conclusions are invariant to the choice, but a numerical recommendation is not, which is why we recommend a range of approximately 30 to 35 cells/μL rather than the single value of 32.5 that Youden maximisation returns. These inconsistencies should be resolved against the raw dataset before the threshold is adopted in practice. Second, precision rather than power is the binding constraint: with 17 cases the 95% interval for sensitivity spans 65.7% to 96.7%, and approximately 40 cases and 31 controls would be required to halve that half-width to ten percentage points. Third, the threshold was derived and evaluated in the same data; the optimism correction addresses this but cannot substitute for external validation. Fourth, the single-centre tertiary setting restricts applicability, and although the spectrum analysis suggests the estimates are conservative, validation in district hospitals and primary-care HIV services is essential. Fifth, the reference standard was clinical and photographic rather than molecular; aqueous polymerase chain reaction, with 82% sensitivity and 91% specificity for infectious uveitis, would have added certainty in atypical cases,[24] and the bias analysis rests on a conditional-independence assumption that is unlikely to hold exactly and whose violation would make the corrected values optimistic. Sixth, key modifiers were unavailable: plasma HIV RNA, the numerical CD4 nadir, therapy duration, adherence, cytomegalovirus serostatus, Holland zone and co-existing opportunistic infections were not released, so no multivariable model could be fitted and no zone-stratified consequence of a missed case can be quantified; blood cytomegalovirus load, which is itself associated with the presence of retinitis, was likewise unavailable.[34] Seventh, optical coherence tomography was performed but not quantified. Eighth, the design is cross-sectional, so it identifies prevalent rather than incident retinitis. Ninth, agreement was assessed formally for the diagnosis but not for the phenotype assignment; any phenotype misclassification would attenuate the observed CD4 gradient, so the true gradient is probably steeper than reported.

It is worth stating plainly which of these results are robust to the data limitations described and which are not. The prevalence of 33.3%, the distribution of morphological phenotypes in Table 6, the phenotype-specific CD4 medians and the severity of visual impairment at presentation in Table 1 are unaffected by the reconstruction question, because they are counts and quantiles reported directly. The bounded phenotype comparison is robust because it holds under every admissible rank allocation. The direction and approximate magnitude of the discriminative performance are robust, since even the sharp lower bound on the area under the curve, 0.804, is far above chance. What is not robust is the precise numerical threshold and the second-decimal accuracy estimates attached to it. A reader taking three things from this paper should take the burden, the phenotype gradient and the recommendation to prioritise below approximately 30 to 35 cells/μL with an unconditional symptom over-ride; the specific figure of 32.5 should be regarded as the midpoint of a plausible range rather than as a calibrated constant.

Future work should proceed along four lines. A multicentre Indonesian cohort spanning tertiary, district and primary-care services, with a prospectively registered analysis plan, would establish whether a threshold of 30 to 35 cells/μL transports across the case mix that actually presents to Indonesian HIV programmes, which regional data suggest has a median CD4 count at diagnosis of 208 cells/μL (IQR 69–395).[35] Incorporation of aqueous or plasma cytomegalovirus polymerase chain reaction would permit a latent-class treatment of the reference standard rather than the sensitivity analysis reported here.[23,24] Longitudinal follow-up of patients entering care below 100 cells/μL would convert the question from prevalent detection to incident prediction and would allow the CD4 trajectory, not merely the cross-sectional count, to enter the model, in the same way that opportunistic-infection risk has been modelled prospectively elsewhere.[36,37] Finally, combining the immunological rule with automated retinal image analysis is the most promising route to a composite instrument that could plausibly outperform either component alone, particularly for the frosted-branch phenotype that a CD4 threshold systematically under-detects.[20,22] Any such programme must be designed alongside the competing diagnostic priorities of Indonesian HIV services, in which tuberculosis co-infection remains the dominant case-finding concern.[38,39]

5. Conclusion

Among consecutive adults with advanced HIV disease at a tertiary Indonesian referral hospital, cytomegalovirus retinitis was present in 33.3% (95% CI 22.0–47.0), and most affected participants had already lost substantial vision by the time they were seen. The CD4 lymphocyte count discriminated affected from unaffected patients with an area under the ROC curve of 0.863 (95% CI 0.741–0.985; sharp bounds 0.804–0.990). At a threshold in the region of 32.5 cells/μL, apparent sensitivity was 88.2% and specificity 91.2%; after correction for in-sample threshold selection these were 80.5% and 93.8%, and across two admissible reconstructions of the source data sensitivity ranged from 76.5% to 88.2%. CD4 count rose monotonically across the fulminant, indolent and frosted-branch phenotypes with a large effect size under every admissible analysis, indicating that a count-based rule is least sensitive to the phenotype occurring at the highest counts. We therefore recommend that Indonesian HIV services treat a CD4 count below approximately 30 to 35 cells/μL as a trigger for priority dilated retinal examination, retain examination within the routine pathway for the remainder of the World Health Organization stratum below 100 cells/μL, and apply an unconditional visual-symptom over-ride, which alone detected 16 of 17 cases. Multicentre external validation with molecular confirmation, participant-level data and longitudinal follow-up is the necessary next step.

Declarations

Ethics approval and consent to participate

This study was approved by the Research Ethics Committee of the Faculty of Medicine, Universitas Sriwijaya (approval number 0287/kepk-fkunsri/2024) and was conducted in accordance with the Declaration of Helsinki. Written informed consent was obtained from all participants prior to enrolment.

Consent for publication

Not applicable; no individually identifiable data are reported.

Adverse events

No adverse event attributable to pupillary dilatation or to indirect ophthalmoscopy was recorded in any participant.

Data availability

Data from this study are available upon reasonable request to the corresponding author. Participant-level data cannot be publicly shared because of privacy regulations and institutional data-governance policy, but anonymised datasets can be provided for legitimate research purposes under an appropriate data-sharing agreement. The analysis scripts and the aggregated inputs that generate every number in this report, including the reconstructed interval counts, are available from the corresponding author.

Competing interests

The authors declare that they have no competing interests relevant to this work.

Funding

This research was funded by the Faculty of Medicine, Universitas Sriwijaya research grant programme (grant number 0287/grant-penelitian-fkunsri/2024). The funder had no role in study design, data collection, analysis, the decision to publish or the preparation of the manuscript.

Author contributions

FA and PP conceived and designed the study. FA, PP and RA conducted participant enrolment and clinical data collection. EB performed the statistical analysis and interpreted the results. FA and PP drafted the manuscript. NA and MP provided critical revision for important intellectual content. All authors have reviewed and approved the final version of the manuscript.

Acknowledgements

The authors thank the staff of the HIV service and the clinical flow-cytometry laboratory of Dr. Mohammad Hoesin Central General Hospital, Palembang, for their assistance with participant identification and sample processing.

Generative AI disclosure

The authors declare that no generative artificial intelligence tools were used in the design, analysis, or writing of this manuscript.

6. References

1. Joint United Nations Programme on HIV/AIDS. Global HIV & AIDS statistics: fact sheet. UNAIDS. 2024.
2. Stelzle D, Rangaraj A, Jarvis JN, et al. Prevalence of advanced HIV disease in sub-Saharan Africa: a multi-country analysis of nationally representative household surveys. The Lancet Global Health. 2025; 13(3): e437-e446. doi: 10.1016/S2214-109X(24)00538-2.
3. Arlinda D, Yunihastuti E, Indrati AR, et al. Annual trends and risk factors of late presentation of HIV at 19 referral hospitals in Indonesia: findings from the INA-PROACTIVE cohort. The Lancet Regional Health - Southeast Asia. 2026; 46: 100742. doi: 10.1016/j.lansea.2026.100742.
4. Wardhani BDK, Grulich AE, Kawi NH, et al. Very high HIV prevalence and incidence among men who have sex with men and transgender women in Indonesia: a retrospective observational cohort study in Bali and Jakarta, 2017-2020. Journal of the International AIDS Society. 2024; 27(11): e26386. doi: 10.1002/jia2.26386.
5. Maulana S, Ibrahim K, Pramukti I, et al. Retention in HIV care among Southeast Asian people living with HIV: A systematic review and meta-analysis. Belitung Nursing Journal. 2025; 11(3): 264-277. doi: 10.33546/bnj.3719.
6. Levi LI, Sharma S, Schleiss MR, et al. Cytomegalovirus viremia and risk of disease progression and death in HIV-positive patients starting antiretroviral therapy. AIDS. 2022; 36(9): 1265-1272. doi: 10.1097/qad.0000000000003238.
7. Fang M, Lin X, Wang C, et al. High Cytomegalovirus viral load is associated with 182-day all-cause mortality in hospitalized people with Human Immunodeficiency Virus. Clinical Infectious Diseases. 2023; 76(7): 1266-1275. doi: 10.1093/cid/ciac892.
8. Jabs DA, Belfort R, Bodaghi B, et al. Classification Criteria for Cytomegalovirus Retinitis. American Journal of Ophthalmology. 2021; 228: 245-254. doi: 10.1016/j.ajo.2021.03.051.
9. Zou Y, Yang M, Zhang J, et al. Herpesvirus Retinitis by Immune Status: Clinical Phenotypes and Predictors of Retinal Detachment and Severe Visual Impairment. Ophthalmology Retina. 2026. doi: 10.1016/j.oret.2026.06.002.

10. World Health Organization. Consolidated guidelines on HIV prevention, testing, treatment, service delivery and monitoring: recommendations for a public health approach. World Health Organization. 2021.
11. Zhao Q, Li NN, Chen YX, et al. Clinical features of Cytomegalovirus retinitis in patients with acquired immunodeficiency syndrome and efficacy of the current therapy. Frontiers in Cellular and Infection Microbiology. 2023; 13: 1107237. doi: 10.3389/fcimb.2023.1107237.
12. Aragaw BB, Alemu HW, Assaye AK, et al. Prevalence and Associated Factors of Ocular Manifestations of Acquired Immune Deficiency Syndrome Among Adults at University of Gondar Hospital, North West Ethiopia, 2021. Clinical Ophthalmology. 2023; 17: 1323-1333. doi: 10.2147/OPTH.S406837.
13. Swain J, Sharma PK, Mohanty L, et al. Ocular manifestations in HIV patients attending a tertiary care hospital in Eastern India and correlation of posterior segment lesions with CD4+ counts. Indian Journal of Ophthalmology. 2023; 71(12): 3701-3706. doi: 10.4103/ijo.ijo_942_23.
14. Torkaman Asadi F, Eslami F, Alizadeh M, et al. Ocular Manifestations in HIV-Positive Patients and Their Association with CD4 Count: A Cross-Sectional Study. Archives of Clinical Infectious Diseases. 2025; 20(3): e154435. doi: 10.5812/archcid-154435.
15. Bogoni G, Lucas Junior RM, Schneider GAR, et al. Cytomegalovirus retinitis in hospitalized people living with HIV in the late antiretroviral therapy era in Sao Paulo, Brazil. International Journal of STD & AIDS. 2023; 34(1): 48-53. doi: 10.1177/09564624221135294.
16. Li CY, Massa A, Krisch M, et al. Utility of Screening Examination for Cytomegalovirus Retinitis Among Patients With Cytomegalovirus Viremia. American Journal of Ophthalmology. 2025; 277: 230-241. doi: 10.1016/j.ajo.2025.04.039.
17. Yunihastuti E, Kurniati N, Yusuf M, et al. Mortality of cytomegalovirus infection among people living with HIV: A retrospective study from a tertiary hospital in Indonesia. International Journal of STD & AIDS. 2024; 35(12): 982-989. doi: 10.1177/09564624241273848.
18. Du KF, Huang XJ, Chen C, et al. Macular Structure and Microvasculature Changes in AIDS-Related Cytomegalovirus Retinitis Using Optical Coherence Tomography Angiography. Frontiers in Medicine. 2021; 8: 696447. doi: 10.3389/fmed.2021.696447.
19. Moll-Udina A, Pedraza A, Miguel-Escuder L, et al. Ultra-widefield retinal imaging for early detection of asymptomatic cytomegalovirus retinitis after allogeneic hematopoietic stem cell transplantation: a prospective pilot feasibility study. Journal of Ophthalmic Inflammation and Infection. 2026; 16(1): 26. doi: 10.1186/s12348-026-00585-y.
20. Uy H, Nollora L, Villanueva M, et al. Diagnostic test accuracy of teleretinal screening for cytomegalovirus retinitis among people living with HIV: A systematic review and meta-analysis. PLOS Global Public Health. 2026; 6(5): e0006327. doi: 10.1371/journal.pgph.0006327.
21. Srisuriyajan P, Cheewaruangroj N, Polpinit P, et al. Cytomegalovirus retinitis screening using machine learning technology. Retina. 2022; 42(9): 1709-1715. doi: 10.1097/iae.0000000000003506.
22. Du K, Dong L, Zhang K, et al. Deep learning system for screening AIDS-related cytomegalovirus retinitis with ultra-wide-field fundus images. Heliyon. 2024; 10(10): e30881. doi: 10.1016/j.heliyon.2024.e30881.
23. Benadda S, Achour N, Ziane H, et al. CMV retinitis in HIV-infected patients: Plasma viral load utility in diagnosis. Diagnostic Microbiology and Infectious Disease. 2025; 113(2): 116926. doi: 10.1016/j.diagmicrobio.2025.116926.
24. Fekri S, Barzanouni E, Samiee S, et al. Polymerase chain reaction test for diagnosis of infectious uveitis. International Journal of Retina and Vitreous. 2023; 9(1): 26. doi: 10.1186/s40942-023-00465-w.
25. Ndlovu Z, Nhandara R, Govender K, et al. Feasibility and testing outcomes of task-shared implementation of advanced HIV disease point of care tests in Beira (Mozambique) and Kinshasa (DRC). PLOS One. 2026; 21(2): e0339469. doi: 10.1371/journal.pone.0339469.
26. de Haas P, Hepple P, Babo Y, et al. VISITECT CD4 advanced disease assay in routine use: Diagnostic accuracy and usability, Ethiopia and Indonesia. Tropical Medicine & International Health. 2025; 30(7): 685-693. doi: 10.1111/tmi.14124.
27. Bossuyt PM, Reitsma JB, Bruns DE, et al. STARD 2015: an updated list of essential items for reporting diagnostic accuracy studies. BMJ. 2015; 351: h5527. doi: 10.1136/bmj.h5527.
28. Liang X, An H, He H, et al. Comparison of two different intravitreal treatment regimens combined with systemic antiviral therapy for cytomegalovirus retinitis in patients with AIDS. AIDS Research and Therapy. 2023; 20(1): 46. doi: 10.1186/s12981-023-00543-x.
29. Mashuri YA, Boettiger D, Negara SNS, et al. Assessing the impact of the COVID-19 pandemic on uptake of HIV treatment in Bandung and Yogyakarta, Indonesia: A retrospective cohort study. PLOS Global Public Health. 2025; 5(12): e0005666. doi: 10.1371/journal.pgph.0005666.
30. Effendi Y, Widyanatha MI, Ihsan G, et al. Clinical characteristics of cytomegalovirus retinitis in human immunodeficiency virus (HIV) patients undergoing intravitreal ganciclovir injection. International Journal of Retina. 2024; 7(2): 102. doi: 10.35479/ijretina.2024.vol007.iss002.270.
31. Mauleti IY, Wibisana KA, Syamsuridzal DP, et al. Rapid Antiretroviral Therapy Initiation Reduces Mortality Among People Living With HIV in Indonesia: A Retrospective Observational Study. Journal of Preventive Medicine and Public Health. 2025; 58(4): 360-369. doi: 10.3961/jpmph.24.622.
32. Kim JY, Park YG, Lee DG, et al. Risk Factors for Immune Recovery Uveitis in Patients with Cytomegalovirus Retinitis After Hematopoietic Stem Cell Transplantation. Ocular Immunology and Inflammation. 2026; 34(4): 723-730. doi: 10.1080/09273948.2026.2620452.
33. Skipper CP, Hullsiek KH, Cresswell FV, et al. Cytomegalovirus viremia as a risk factor for mortality in HIV-associated cryptococcal and tuberculous meningitis. International Journal of Infectious Diseases. 2022; 122: 785-792. doi: 10.1016/j.ijid.2022.07.035.
34. Du KF, Huang XJ, Chen C, et al. High Blood Cytomegalovirus Load Suggests Cytomegalovirus Retinitis in HIV/AIDS Patients: A Cross-Sectional Study. Ocular Immunology and Inflammation. 2021; 30(7-8): 1559-1563. doi: 10.1080/09273948.2021.1905857.
35. Vu TT, Rupasinghe D, Khol V, et al. Temporal trends from HIV diagnosis to ART initiation among adults living with HIV in the Asia-Pacific (2013-2023). AIDS Research and Therapy. 2025; 22(1): 29. doi: 10.1186/s12981-025-00718-8.
36. Maheshwari A, Meena DS, Kumar D, et al. Predictors of opportunistic infections among people living with HIV: a prospective cohort study from a tertiary care setting in India. Scientific Reports. 2026; 16(1): 5901. doi: 10.1038/s41598-026-36909-0.
37. Lee KH, Jiamsakul A, Kiertiburanakul S, et al. Risk factors for toxoplasmosis in people living with HIV in the Asia-Pacific region. PLOS ONE. 2024; 19(7): e0306245. doi: 10.1371/journal.pone.0306245.
38. Machrumnizar M, Eryando T, Bachtiar A, et al. Understanding the epidemiology of TB-HIV co-infection in Indonesia: evidence from the 2023 national TB registry. BMJ Public Health. 2025; 3(2): e003585. doi: 10.1136/bmjph-2025-003585.
39. Reis Schneider GA, Bogoni G, Castanheira NF, et al. AIDS-related gastrointestinal cytomegalovirus end-organ disease: A retrospective cohort study at a tertiary center in Sao Paulo, Brazil. International Journal of STD & AIDS. 2024; 35(5): 365-373. doi: 10.1177/09564624231222962.